

# Electronic structure and optical properties of layered perovskites $\text{Sr}_2\text{MO}_4$ ( $M=\text{Ti, V, Cr, Mn and Co}$ ): *ab initio* study

Hongming Weng,<sup>1,\*</sup> Y. Kawazoe,<sup>1,†</sup> Xiangang Wan,<sup>2</sup> and Jinming Dong<sup>2,‡</sup>

<sup>1</sup>*Institute for Materials Research, Tohoku University, Sendai 980-8577, Japan*

<sup>2</sup>*Group of Computational Condensed Matter Physics,*

*National Laboratory of Solid State Microstructures and Dept. of Physics,*

*Nanjing University, Nanjing 210093, P. R. China*

(Dated: April 12, 2019)

A series of layered perovskites  $\text{Sr}_2\text{MO}_4$  ( $M=\text{Ti, V, Cr, Mn and Co}$ ) are studied by *ab initio* calculations within generalized gradient approximation (GGA) and GGA+ $U$  ( $U$  is the on site Coulomb interaction) method. The total energies for different magnetic states, the non-magnetic (NM), ferromagnetic (FM), the layered anti-ferromagnetic state with alternating ferromagnetic plane (AFM-I) and the staggered in-plane antiferromagnetic (AFM-II) order, are calculated.  $\text{Sr}_2\text{TiO}_4$  is always a non-magnetic band insulator. AFM-II insulator state has the lowest total energy within both GGA and GGA+ $U$  for  $\text{Sr}_2\text{MnO}_4$ , in consistent with the experimental measurements. While the GGA is not enough for getting the experimentally observed AFM-II insulating states for  $M=\text{V}$  and Cr cases. Though GGA+ $U$  could give a stable AFM-II state after a critical value of  $U$  ( $U_c$ ), the optical conductivity spectra in that state show that only electron-electron correlation is not enough for describing the real electronic states in  $\text{Sr}_2\text{VO}_4$  and  $\text{Sr}_2\text{CrO}_4$ . Some kinds of proper cooperative ligand field changes are needed.

## I. INTRODUCTION

Layered perovskites have attracted intensive study because they show various intriguing physical properties such as high- $T_c$  superconductivity in cuprates and  $\text{Sr}_2\text{RuO}_4$ <sup>1</sup> and spin/charge stripe in nickelates.<sup>2</sup> Recently, a series layered perovskites  $\text{Sr}_2\text{MO}_4$  ( $M=\text{Ti, V, Cr, Mn and Co}$ ) are successfully synthesized for studying the variation of the electronic structure depending on the increasing of  $d$  electrons from zero ( $d^0$  for  $\text{Ti}^{4+}$ ) to half-filled ( $d^5$  for  $\text{Co}^{4+}$ ).<sup>3</sup> The physical properties do vary largely with the change of  $d$  electron number. In  $d^0$  case, the  $\text{Sr}_2\text{TiO}_4$  is always a non-magnetic band insulator. For  $M=\text{V}$ , it is thought that the surrounding elongated octahedral crystal field will make the  $d^1$  electron stay in the double degenerate  $d_{yz+zx}$  orbit, which is orbital active and is expected to have some kind of orbital ordering.<sup>4</sup> In Cr case, two  $d$  electrons is supposed to occupy the double degenerate  $d_{yz+zx}$  orbit and is thought to be a simple Mott-Hubbard AFM-II insulator. Three  $d$  electrons in  $\text{Sr}_2\text{MnO}_4$  will take the three low Hubbard band composed by the  $t_{2g}$  orbital leading the system to be an AFM-II insulator. For  $M=\text{Co}$ , the first-principles calculation<sup>5</sup> shows that the strong Co 3d-O 2p hybridization makes the  $d^5$  system be a FM metal. All these systematically variation of the electronic structure are revealed by the optical conductivity measurements.<sup>3</sup> The anisotropy of the optical conductivity due to the 2-dimensional  $\text{MO}_2$  sheets in the layered perovskite structure is also clearly shown by the polarized measurement with  $E \perp c$  and  $E \parallel c$ .

To understand more of these systems, we employ the first principles calculation to investigate the details of electronic structure and optical conductivity spectra for these layered perovskite systems in this paper. We find that GGA is not enough for predicting the correct ground

state of  $\text{Sr}_2\text{VO}_4$  and  $\text{Sr}_2\text{CrO}_4$ . The former had been already carefully investigated by the local spin density approximation (LSDA) calculation since it has a dual relation to the one 3d hole per Cu sites ( $d^9$  system) in the parent compounds of the cuprate superconductors  $\text{La}_2\text{CuO}_4$ , which has the same  $\text{K}_2\text{NiF}_4$  structure.<sup>6</sup> But the LSDA calculation failed in reproducing the AFM-II insulator state. The  $\text{Sr}_2\text{CrO}_4$  is discovered to be semiconductor, in contrary to the metallic cubic perovskite  $\text{SrCrO}_3$ . If ignoring the empty  $e_g$  orbital, this  $t_{2g}$   $d^2$  system also has the dual relation to the  $d^4$  system ( $\text{Sr}_2\text{RuO}_4$ ), which has two holes in narrow  $t_{2g}$  bands showing superconductivity. To take into account the on-site electron-electron correlation effects, GGA+ $U$  calculations are performed on these two systems. Increasing with  $U$ , the AFM-II state becomes more stable related to the FM and AFM-I state. The critical value  $U_c$  is found to be about 2.08 and 3.36 eV for  $M=\text{V}$  and Cr, respectively. But the optical conductivity spectra calculation show that the Mott-Hubbard gap is overestimated in both cases by using such  $U$  values. Further analysis shows that in  $M=\text{V}$  and Cr systems, only including the electron-electron correlation effect is not enough, a proper ligand field changes which acts in cooperation with  $U$  to further split the  $t_{2g}$  bands is also necessary for properly reproducing the electronic structures and other properties. Both GGA and GGA+ $U$  calculations indicate that the AFM-II state is stable for  $\text{Sr}_2\text{MnO}_4$  system and its optical conductivity is also discussed. For  $M=\text{Co}$ , we just do some calculations for proper checking of some settings since the intense *ab initio* study of  $\text{Sr}_2\text{CoO}_4$  had been performed in Ref. 5.

## II. METHODOLOGY

The plane wave basis VASP code<sup>7</sup> has been employed for our calculations, in which the PAW version of pseudopotentials<sup>8</sup> within GGA of Perdew and Wang is used to represent the core electrons. Dudarev's approach for  $+U$  is used in the GGA+ $U$  calculation, in which only one effective on-site Coulomb interaction parameter is needed.<sup>9</sup> By ignoring the slight orthorhombic deviation from the tetragonal symmetry in the first approximation,<sup>5</sup> all the  $\text{Sr}_2\text{MO}_4$  are assumed to have the typical  $\text{K}_2\text{NiF}_4$  structure with tetragonal space group  $I4/mmm$ , and the lattice parameters are taken from the experimental measurements of the thin film samples<sup>3</sup> as shown in Table. I. The internal atomic coordinations are fully optimized until the force on the atom is less than  $0.002 \text{ eV}/\text{\AA}$ . For every case, various magnetic configuration are considered in order to find the ground state though in experiments the 3-dimensional ferromagnetism or layered AFM state with alternating ferromagnetic  $\text{MO}_2$  sheets (AFM-I) are both ruled out from the thin film samples for  $M=\text{V, Cr and Mn}$ .<sup>3</sup> The typical and simplest staggered in-plane antiferromagnetism<sup>10</sup> for layered perovskite structure is labelled as AFM-II state. For simulating the AFM-II state, a cell as large as  $\sqrt{2} \times \sqrt{2} \times 1$  of the conventional  $\text{K}_2\text{NiF}_4$  unit cell is needed, which is also used for other states.

The inter-band optical responses are calculated within the electric-dipole approximation using the Kubo formula<sup>11</sup> implemented by J. Furthmüller,<sup>12</sup> in which the imaginary part of the dielectric function can be expressed as

$$\varepsilon_2(\omega) = \frac{8\pi^2 e^2}{\omega^2 m^2 V} \sum_{c,v} \sum_k | \langle c, k | \hat{\mathbf{e}} \cdot \mathbf{p} | v, k \rangle |^2 \times \delta[E_c(k) - E_v(k) - \hbar\omega],$$

where  $c$  and  $v$  represent the conduction and valence bands, respectively.  $|\langle c, k \rangle|$  and  $E_c(E_v)$  are the eigenstates and eigenvalue of conduction (valence) band obtained from the VASP calculations.  $\mathbf{p}$  is the momentum operator,  $\hat{\mathbf{e}}$  is the incident photon's electric field vector denoting the polarization of the light, and  $\omega$  is the frequency of incident photon. An  $8 \times 8 \times 8$  grid is used to sample the Brillouin zone for the integration of  $k$ -space with the linear tetrahedron scheme improved by Blöchl *et al.*<sup>13</sup> The energy cutoff for the plane wave is 520 eV. The convergency on  $k$ -points and energy cutoff is carefully checked.

## III. RESULT AND DISCUSSION

The optimized crystal structure parameters for  $\text{Sr}_2\text{MO}_4$  are listed in Table I. For  $\text{Sr}_2\text{TiO}_4$ , Fennie *et al.* reported the internal parameters are 0.160 and 0.145 for apical oxygen ( $\text{O}_a$ ) and Sr atoms, respectively, by the LDA calculation.<sup>14</sup> The experimental internal parameters for  $\text{O}_a$  and Sr atom in  $\text{Sr}_2\text{VO}_4$  are 0.15778 and

TABLE I: The lattice parameter and optimized internal coordinates of the apical oxygen ( $\text{O}_a$ ) and Sr atoms relative to the  $c$  lattice.

	Ti	V	Cr	Mn	Co
a	3.866	3.832	3.756	3.755	3.755
c	12.60	12.59	12.59	12.62	12.52
$\text{O}_a$	0.15950	0.15781	0.15899	0.15858	0.15717
Sr	0.14589	0.14486	0.14673	0.14646	0.14410
$d_{ab}$	1.93	1.92	1.88	1.88	1.88
$d_c$	2.01	1.99	2.00	2.00	1.98
$J$	1.041	1.036	1.063	1.063	1.053

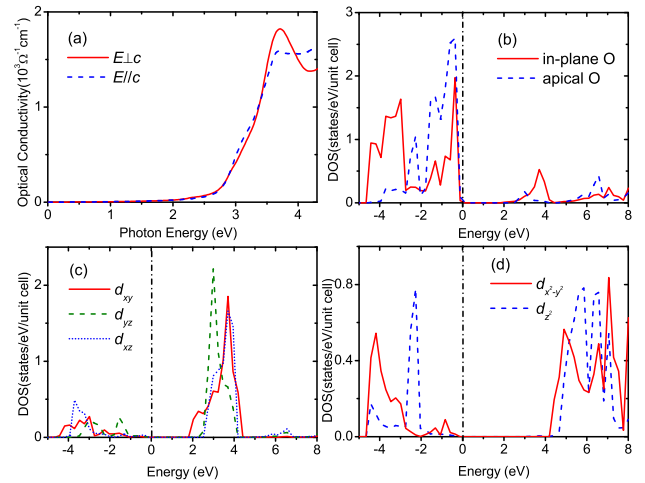


FIG. 1: (color online). (a) Optical conductivity spectrum, (b) projected partial DOS for in-plane (solid) and apical (dashed) oxygen 2p bands and Ti 3d (c)  $t_{2g}$  and (d)  $e_g$  bands calculated within GGA for  $\text{Sr}_2\text{TiO}_4$ . The vertical dash-dotted line indicates the Fermi energy level.

0.14562.<sup>15</sup> For  $\text{Sr}_2\text{CoO}_4$ , Matsuno *et al.* gave those obtained by LSDA calculation as 0.15778 and 0.14562.<sup>5</sup> All of these are well comparable with ours. This means the energy cutoff and the  $k$ -point sampling are good enough, and the crystal field effects are well considered in our calculations. It is found that in all cases, the oxygen octahedron surrounding the  $M$  has the Jahn-Teller (JT) distortion elongated along the  $c$ -axis by different degree, which is defined as  $J=d_c/d_{ab}$  with  $d_c$  ( $d_{ab}$ ) denoting the M-O bond length along the  $c$ -axis (in the  $ab$  plane).

The  $\text{Sr}_2\text{TiO}_4$  system is very simple. It is a band insulator as shown by the density of states (DOS) in Fig. 1. The valance bands are mostly oxygen 2p electrons and the conduction band are Ti's empty 3d orbital. The band width of  $t_{2g}$  is much narrower than that of  $e_g$  band due to the different bonding type when hybridized with the oxygen  $p$  bands. Also, the in-plane  $d_{xy}$  and  $d_{x^2-y^2}$  bands are wider than the counterpart out of the plane because of the elongated oxygen octahedra. The optical conductivities for the incident photon with electric field  $E$  parallel to the  $c$ -axis ( $E\parallel c$ ) and perpendicular to the

$c$ -axis ( $E \perp c$ ) are also shown. The anisotropy due to the 2-dimensional layered structure is observable though the difference is not so large. Compared with the experimental value, the optical gap is underestimated due to the well-known shortcomings of GGA.<sup>16</sup> The shoulder near 3.0 eV in  $E \parallel c$  is due to the transition from apical oxygen  $2p$  orbital to the  $d_{yz}$  centering at 3.0 eV. Such a kind of transition is not shown for  $E \perp c$ . In  $E \perp c$  and  $E \parallel c$ , the peak around 3.7 eV is attributed to the transition from apical and in-plane oxygen  $2p$  orbital to the  $d_{xz}$  and  $d_{xy}$  orbital around 3.7 eV above the Fermi level. The quite broader peak in  $E \parallel c$  is due to the broader  $2p$  DOS structure of apical oxygen than that of in-plane oxygen below the Fermi level as shown in the partial DOS.

For  $M=V$ , Cr, Mn and Co, since the  $d$  bands are partially occupied, the spin order degree of freedom should be taken into account for the studying.  $Sr_2CoO_4$  had been intensively studied in Ref. 5, and we will not cover this again. But by using the parameters given above, our calculations show that the FM state is lower than the non-magnetic state by about 297 meV/cell for  $Sr_2CoO_4$ , the same as that given in Ref. 5. For searching the ground state of the others, the total energy for various magnetic state related to the FM state with the optimized structure has been calculated within GGA as shown in Table II. Obviously, the ground state for  $Sr_2MnO_4$  is correctly predicted as AFM-II state, while for  $M=V$  and Cr the results show they are in the AFM-I state, which is not the case as proposed by the experimental analysis. In fact, the FM order in the  $ab$ -plane would result metallic optical conductivity when  $E \perp c$  though the insulating state in  $c$  direction might be maintained. Generally, it is thought that in the layered perovskite the coupling between the  $MO_2$  sheets could be ignored. In Fig. 2, the DOS for AFM-I state of  $Sr_2VO_4$  and  $Sr_2CrO_4$  clearly show the metallic features. Though the elongated oxygen octahedral crystal field makes the double degenerate  $d_{yz+xz}$  orbital lower than the  $d_{xy}$  orbital, there are three bands cross the Fermi level for  $d^1$  and  $d^2$  system when  $M=V$  and Cr, respectively. This is very similar to that in  $Sr_2RuO_4$   $d^4$  system having the same layered structure.<sup>17</sup> One thing should be mentioned is that when  $M=V$ , the AFM-II state is not achieved in our GGA calculation even initially the magnetic moment on V ions are set as AFM-II configuration, the electronic density always converges to the NM state. So, the AFM-II energy for  $M=V$  listed in Table II is that of NM state. W. E. Pickett *et al.* had also tried to search for the AFM state in LSDA calculation for  $Sr_2VO_4$  but failed.<sup>6</sup>

For the  $d$  electron system, it is naturally to introduce the strong electron-electron correlation  $U$  into the calculation to remedy the deficiency of GGA. It had been shown to be effective when predicting the correct energy order for the  $t_{2g}$  band perovskite  $YTiO_3$  where GGA failed.<sup>18</sup> For searching the proper parameter  $U$ , we do a series calculation for  $M=V$  and Cr in different magnetic states. The total energy related to the FM state developed with the  $U$  values is shown in Fig. 3. For

TABLE II: The total energy related to the FM state for various magnetic state in  $Sr_2MO_4$  with  $M=V$ , Cr, and Mn calculated within GGA. The energy unit is in meV/cell.

	V	Cr	Mn
NM	280.9	1252.4	3312.6
FM	0.0	0.0	0.0
AFM-I	-6.0	-29.4	-38.5
AFM-II	280.0	297.8	-629.8

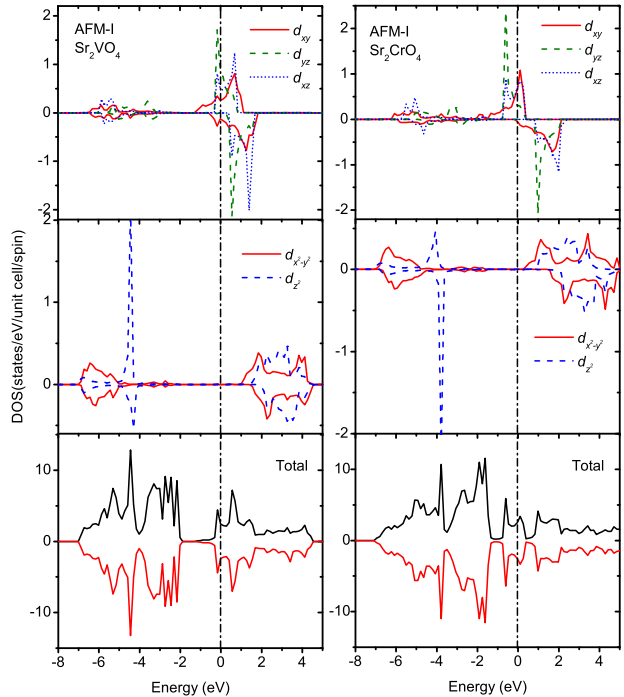


FIG. 2: (color online). The calculated DOS of AFM-I state for  $M=V$  (left panel) and Cr (right panel).

$M=V$ , the AFM-I state is nearly degenerate with the FM state indicating the coupling between the  $VO_2$  sheets is very small and could be ignorable. But for  $M=Cr$ , the AFM-I state is more stable than the FM state and the energy difference is nearly independent of the  $U$  parameter. Perhaps the  $c$  lattice parameter of  $Sr_2CrO_4$  used here from the experimental sample is smaller because of the strain of substrate, which results the  $CrO_2$  sheets are close enough to feel each other. But in experiments, for both  $M=V$  and Cr, the suggested magnetic structure is the AFM-II configuration, whose total energy will be the lowest when  $U$  is larger than the critical value  $U_c$ ,  $\sim 2.08$  and  $\sim 3.36$  eV for  $M=V$  and Cr, respectively, as shown in Fig. 3. The  $U_c$  is larger than the corresponding  $t_{2g}$  band width, so  $Sr_2VO_4$  and  $Sr_2CrO_4$  are strong correlated narrow band systems, the including of  $U$  is necessary for studying these two systems.

In Fig. 4, we show the evolving of the  $t_{2g}$  DOS for  $M=V$  and Cr with the  $U$  parameter in the AFM-II state.

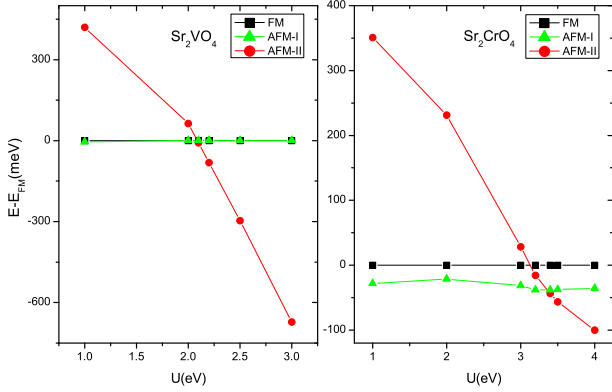


FIG. 3: (color online). The change of the total energy related to the FM state as the  $U$  parameter for  $M=V$  and Cr.

In  $\text{Sr}_2\text{VO}_4$ , the electrons will shift from  $d_{xz+yz}$  to  $d_{xy}$  as the  $U$  increase, making the hybridization between them less. The metal to insulator transition happens near the  $U=2.0$  eV with the  $d_{xy}$  separated from the  $d_{yz+xz}$  orbital. So, the one  $d$  electron mostly occupy the spin-up  $d_{xy}$  orbital instead of the doubly degenerate  $d_{yz+xz}$  in the picture of elongated JT distortion. This kind of occupancy will kill the degree of freedom of orbital ordering though recently Y. Imai *et al.* had proposed a kind of orbital-stripe order.<sup>4</sup> In fact, when in the FM state, the doubly degenerate  $d_{yz+xz}$  occupied by one  $d$  electron will cause the FM-instability as found by W. E. Pickett *et al.*<sup>6</sup> In contrary, in  $\text{Sr}_2\text{CrO}_4$ , the two  $d$  electrons on the  $\text{Cr}^{4+}$  ion will occupy the  $d_{yz+xz}$  orbital with  $d_{xy}$  empty as the  $U$  increasing. The metal-insulator transition will happen at a higher  $U$  about 5.0 eV (not shown here) where the  $d_{xy}$  orbital is totally separated from the  $d_{yz+xz}$  orbital. Here, the  $d_{yz+xz}$  is lower than the  $d_{xy}$  in consistent with the elongated JT distortion of the oxygen octahedron. So, in the  $M=V$  and Cr case, the competition between the JT distortion and  $U$  are totally different. In the former case, the  $U$  acts oppositely against the JT distortion, while in the latter case, they work together cooperatively, which can also be seen from the force on the apical oxygen atoms. Before the metal-insulator transition, as the  $U$  increase, the apical oxygen atoms in  $M=V$  case will feel an increasing flatten force, while in  $M=\text{Cr}$ , the force is going to elongate the octahedron. So, in these two systems, the subtle balance due to the competition between electron-electron correlation and the electron-lattice interaction is key to their physical properties.

Just as an attempt to show the cooperation of JT distortion and the  $U$  effects on the  $\text{Sr}_2\text{CrO}_4$  system, we artificially elongate the oxygen octahedron to a degree of JT distortion being  $J=1.14$  with  $d_{ab}$  fixed. Again, the total energies of various magnetic structure related to the FM state in different  $U$  value is shown in Fig. 5. Obviously, the AFM-II state becomes the most stable when  $U$  is larger than the  $U_c$ , 2.74 eV, which is smaller than the original one, 3.36 eV. So, in the cooperation of

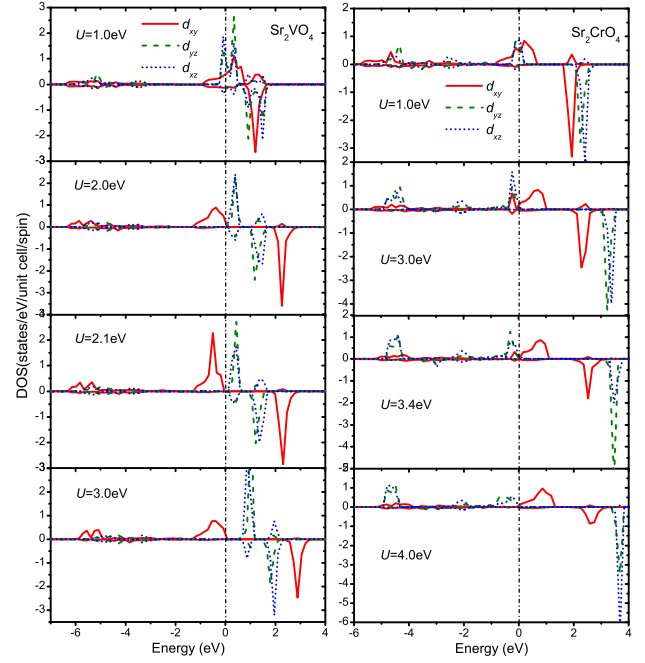


FIG. 4: (color online). The change of the  $t_{2g}$  density of states in the AFM-II state with  $U$  parameter for  $M=V$  (left panel) and Cr (right panel).

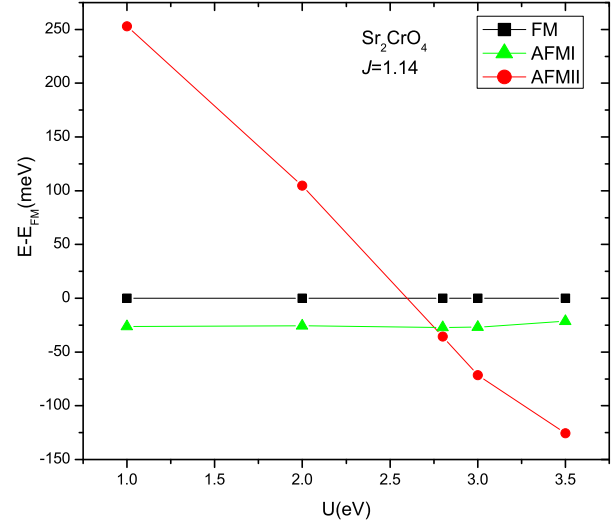


FIG. 5: (color online). The change of the total energy related to the FM state as the  $U$  parameter for  $M=\text{Cr}$  with the JT distortion  $J=1.14$ .

JT distortion, the metal-insulator transition is speedup with the increasing of  $U$ . The splitting of the triply degenerated  $t_{2g}$  is key to such a transition and the realization of AFM-II insulator state for  $\text{Sr}_2\text{VO}_4$  and  $\text{Sr}_2\text{CrO}_4$ . In addition, M. Mochizuki *et al.* had shown that the  $\text{GdFeO}_3$ -type distortion also plays an important role in  $\text{RTiO}_3$  by lifting the degenerated  $t_{2g}$  orbital.<sup>19</sup> The metal

to insulator and FM to AFM transitions could be triggered by increasing the splitting of  $t_{2g}$  orbitals. Since the  $\text{GdFeO}_3$ -type distortion is the generic phenomenon in perovskites, perhaps it is also very important to the  $t_{2g}$  system studied here. The detailed geometry structure information is necessary and important for correctly predicting the ground states. Z. Fang *et al.* has shown that in  $\text{Ca}_{2-x}\text{Sr}_x\text{RuO}_4$ , the detailed structure is crucial for interpretation of its magnetic phase diagram and orbital physics in it.<sup>20</sup>

Since the reported Néel temperature for  $\text{Sr}_2\text{VO}_4$  is about 47 K,<sup>21</sup> the energy difference between the AFM-II and FM states should not be too large if using the popular spin-1/2 2-dimensional Heisenberg model to estimate the Néel temperature.<sup>22</sup> So, according to Fig. 3, roughly, we take the  $U$  value of 2.1 and 3.4 for  $M=\text{V}$  and Cr, a little larger than the critical value, respectively, in the optical properties calculation by using our optimized geometry. The calculated optical conductivity spectra for  $M=\text{V}$  and Cr are shown in Fig. 6 and Fig. 7, respectively. Though in total energy, with the above  $U$  values, the AFM-II state is most stable in energy for  $M=\text{V}$  and Cr, the calculated optical conductivity spectra are to some extent dissimilar with the experimental ones. The fundamental gap from the DOS shown in Fig. 6 for  $\text{Sr}_2\text{VO}_4$  is 0.1 eV. But in the optical conductivity spectrum, the optical gap is as high as about 2.0 eV. Obviously, the transition from the occupied  $d_{xy}$  to the empty  $d_{yz+xz}$  is forbidden when  $E \perp c$ , which is reasonable according to the optical selection rule of  $d - d^*$  transition.<sup>23</sup> According to this, in the AFM-II configuration, the transition from the occupied spin-up  $d_{xy}$  orbital to the nearest neighbors unoccupied spin-up  $d_{xy}$  orbital is allowed, which corresponds to the Mott-Hubbard transition in the optical conductivity. Clearly, the shoulder near the first peak around 3.0 eV is ascribed to such a kind of transition as indicated by the  $t_{2g}$  DOS in Fig. 6 though the energy of this transition is overestimated by using  $U$  as large as 2.1 eV compared with the experimentally suggested  $\sim 1.0$  eV.<sup>3</sup> The first peak around 3.0 eV is ascribed to the transition from the in-plane oxygen 2p bands to the  $d_{yz+xz}$  orbitals centering the 0.5 eV, which is nearly the same as that given by the experiment. When  $E \parallel c$ , due to the existence of SrO layers, the intersite  $d - d^*$  transition is negligible and not seen. The charge transfer in this situation is due to the transition from the apical oxygen 2p to the  $d_{yz+xz}$ . So, the peak is a little higher than that for  $E \perp c$  since the 2p orbital of apical oxygen is a little lower in energy than that of the in-plane one as shown in the DOS. Also, the intensity is a little lower due to the number of states for apical oxygen is less than the in-plane one in one cell. For  $M=\text{Cr}$ , the optical selection rule is also effective and takes responsibility for the semiconducting optical conductivity as shown in Fig. 7. According to this rule, the intersite  $d - d^*$  transition could occur for  $E \perp c$  near the energy of 3.5 eV as indicated by the  $t_{2g}$  DOS. The quite broad peak around 2.5 eV should be ascribed to the charge transfer transition from the in-plane oxygen

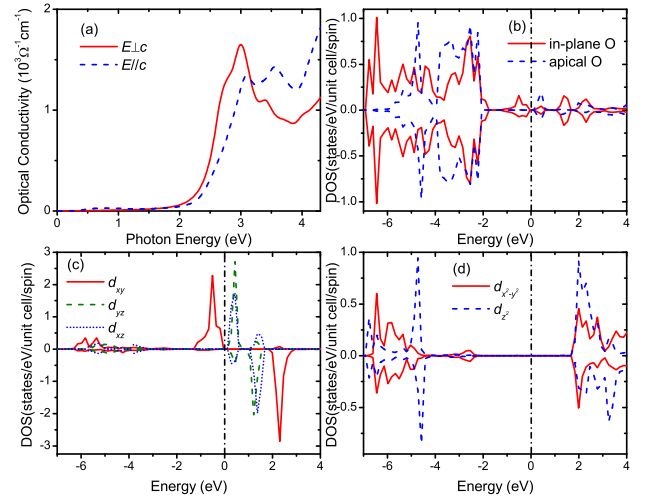


FIG. 6: (color online). The calculated (a) optical conductivity spectrum, (b) in-plane (solid) and apical (dashed) oxygen 2p partial DOS, V 3d (c)  $t_{2g}$  and (d)  $e_g$  partial DOS with  $U=2.1$  eV for  $\text{Sr}_2\text{VO}_4$ .

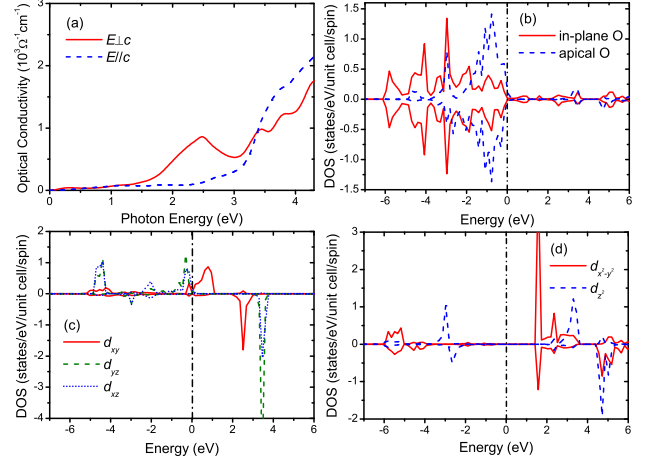


FIG. 7: (color online). The calculated (a) optical conductivity spectrum, (b) in-plane (solid) and apical (dashed) oxygen 2p partial DOS, Cr 3d (c)  $t_{2g}$  and (d)  $e_g$  partial DOS with  $U=3.4$  eV for  $\text{Sr}_2\text{CrO}_4$ .

2p bands near -1.0 eV to the empty  $d_{x^2-y^2}$  orbital at 1.5 eV. The small optical conductivity lower than 2.0 eV could be ascribed to the transition of intra  $d_{xy}$  transitions. So, here the Mott-Hubbard gap is larger than that of the charge transfer gap. The  $U$  of 3.4 eV is too large to locate the energy level of upper Hubbard bands. When  $E \parallel c$ , the charge transfer gap is shifted to higher energy around 3.5 eV, since the  $d_{z^2}$  orbital is higher than the  $d_{x^2-y^2}$  orbital as shown in the DOS.

So, comparing with the experimental spectra,<sup>3</sup> the calculated optical conductivity spectra of  $\text{Sr}_2\text{VO}_4$  and  $\text{Sr}_2\text{CrO}_4$  are not good enough due to the overestimation of Mott-Hubbard and charge transfer transition. As discussed above, only taking into account of the electron-

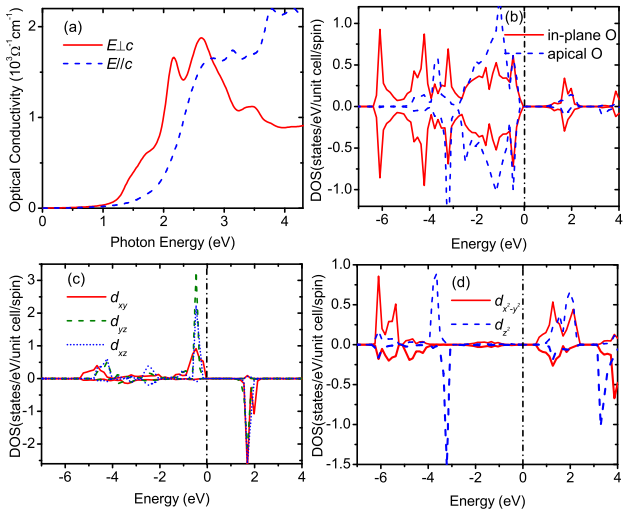


FIG. 8: (color online). The calculated (a) optical conductivity spectrum, (b) in-plane (solid) and apical (dashed) oxygen  $2p$  partial DOS, Mn  $3d$  (c)  $t_{2g}$  and (d)  $e_g$  partial DOS within GGA for  $\text{Sr}_2\text{MnO}_4$ .

electron correlation is not enough for getting the correct ground state for  $\text{Sr}_2\text{VO}_4$  and  $\text{Sr}_2\text{CrO}_4$  systems. Some other factors from the electron-lattice interaction, such as proper JT (flatten in  $M=\text{V}$  and elongate in  $M=\text{Cr}$ ) or  $\text{GdFeO}_3$ -type distortion, acting cooperatively with the electron-electron correlation interaction is expected. For this, the detailed geometries from experimental measurements are needed.

In the  $M=\text{Mn}$  case, both GGA and GGA+ $U$  calculation can predict the correct ground state to be in AFM-II configuration. Three  $d$  electrons on  $\text{Mn}^{4+}$  ion occupy the three lower Hubbard bands with the upper ones empty as shown in Fig. 8. When  $E \perp c$ , the optical gap is due to the transition from in-plane oxygen  $2p$  orbital to the empty Mn  $d_{x^2-y^2}$  orbital around 1.0 eV, which contributes to the first shoulder around 1.5 eV. The narrow peak around

2.2 eV comes from the intersite  $d-d^*$  transition as shown in the Fig. 5(c), which is not discussed in the experimental measurements.<sup>3</sup> The peak around 2.6 eV is due to the transition from the in-plane oxygen  $2p$  bands to the  $t_{2g}$  and  $d_{x^2-y^2}$  near 2.0 eV. When  $E \parallel c$ , the charge transfer transition from the apical oxygen  $2p$  bands to the Mn empty  $d_{z^2}$  orbital contributes most of the spectrum.

#### IV. CONCLUSION

In summary, the electronic structure and the optical conductivity spectra are studied for a series of layered perovskites  $\text{Sr}_2\text{MO}_4$  ( $M=\text{Ti}, \text{V}, \text{Cr}, \text{Mn}$  and  $\text{Co}$ ) by the first principles calculations within GGA and GGA+ $U$ . The GGA calculation could successfully predict the ground state for  $M=\text{Ti}, \text{Mn}$ , and  $\text{Co}$ , but failed in  $M=\text{V}$ , and  $\text{Cr}$ . For the strong correlated  $t_{2g}$  system, GGA+ $U$  could give the most stable state to be AFM-II configuration as suggested by the experimental measurement after a critical value  $U_c$ , about 2.08 and 3.36 eV for  $M=\text{V}$  and  $\text{Cr}$ , respectively. But the optical conductivity spectra show that in both cases, the  $U$  is overestimated. Analysis indicates that some changes in ligand field such as JT or  $\text{GdFeO}_3$ -type distortions might have the key effects on the electronic structures by inducing further splitting of degenerated  $t_{2g}$  orbitals as  $U$  does, which is shown to be critical for the metal-insulator transition and stabilization of AFM-II configuration both in  $\text{Sr}_2\text{VO}_4$  and  $\text{Sr}_2\text{CrO}_4$  systems.

#### Acknowledgments

The authors thank the staff of the Center for computational Materials Science at the IMR for their support and the use of Hitachi SR8000/64 supercomputing facilities. H. M. Weng acknowledge the kind hospitality at IMR and Dr. P. Murugan for discussion.

\* Corresponding author E-mail:hongming@imr.edu

† Electronic address:kawazoe@imr.edu

‡ Electronic address:jdong@nju.edu.cn

<sup>1</sup> Y. Maeno, H. Hashimoto, K. Yoshida, S. Nishizaki, T. Fujita, J. G. Bednorz, and F. Lichtenberg, *Nature (London)* **372**, 532 (1994).

<sup>2</sup> Yoshinori Tokura, *Physics Today* **56**, 50 (2003).

<sup>3</sup> J. Matsuno, Y. Okimoto, M. Kawasaki, and Y. Tokura, *Phys. Rev. Lett.* **95**, 176404 (2005).

<sup>4</sup> Yoshiaki Imai, Igor Solovyev, and Masatoshi Imada, *Phys. Rev. Lett.* **95**, 176405 (2005).

<sup>5</sup> J. Matsuno, Y. Okimoto, Z. Fang, X. Z. Yu, Y. Matsui, N. Nagaosa, M. Kawasaki, and Y. Tokura, *Phys. Rev. Lett.* **93**, 167202 (2004).

<sup>6</sup> W. E. Pickett, D. Singh, D. A. Papaconstantopoulos, H. Krakauer, M. Cyrot and F. Cyrot-lackmann, *Physica C*

**162-164**, 1433 (1989).

<sup>7</sup> G. Kresse and J. Hafner, *Phys. Rev. B* **47**, 558 (1993); *ibid.* **49**, 14 251 (1994); G. Kresse and J. Furthmüller, *Comput. Mat. Sci.* **6**, 15 (1996); G. Kresse and J. Furthmüller, *Phys. Rev. B* **54**, 11 169 (1996).

<sup>8</sup> G. Kresse and D. Joubert, *Phys. Rev. B* **59**, 1758 (1999).

<sup>9</sup> S. L. Dudarev, G. A. Botton, S. Y. Savrasov, C. J. Humphreys and A. P. Sutton, *Phys. Rev. B* **57**, 1505 (1998).

<sup>10</sup> Hongming Weng, Xiangang Wan, Jian Zhou, and Jinming Dong, *Eur. Phys. J. B* **35**, 217 (2003).

<sup>11</sup> B. Adolph, J. Furthmüller, and F. Bechstedt, *Phys. Rev. B* **63**, 125108 (2001).

<sup>12</sup> <http://www.freeware.vasp.de/VASP/>.

<sup>13</sup> Peter E. Blöchl, O. Jepsen, O. K. Andersen, *Phys. Rev. B* **49**, 16223 (1994).

<sup>14</sup> Craig J. Fennie and Karin M. Rabe, Phys. Rev. B **68**, 184111 (2003).

<sup>15</sup> M. Cyrot, B. Lambert-Andron, J.L. Soubeyroux, M. J. Rey, Ph. Dehauht, F. Cyrot-Lackmann, G. Fourcaudot, J. Beille and J. L. Tholence, J. Solid State Chem. **85**, 321 (1990); M. J. Rey, Ph. Dehauht, J. C. Joubert, B. Lambert-Andron, M. Cyrot and F. Cyrot-Lackmann, J. Solid State Chem. **86**, 101 (1990).

<sup>16</sup> R. M. Dreizler and E. K. U. Gross, *Density Functional Theory, An Approach to the Quantum Many-Body Problem* (Springer-Verlag, Berlin, 1990).

<sup>17</sup> V. I. Anisimov, I. A. Nekrasov, D. E. Kondakov, T. M. Rice, and M. Sigrist, Eur. Phys. J. B **25**, 191 (2002).

<sup>18</sup> H. Sawada, K. Terakura, Phys. Rev. B **58**, 6831 (1998).

<sup>19</sup> Masahito Mochizuki and Masatoshi Imada, Phys. Rev. Lett. **91**, 167203 (2003); E. Pavarini, A. Yamasaki, J. Nuss and O. K. Anderson, New J. Phys. **7**, 188 (2005).

<sup>20</sup> Zhong Fang, Kiyoyuki Terakura and Naoto Nagaosa, New J. Phys. **7**, 66 (2005).

<sup>21</sup> A. Nozaki, H. Yoshikawa, T. Wada, H. Yamauchi, and S. Tanaka, Phys. Rev. B **43**, 181 (1991).

<sup>22</sup> Xiangang Wan, M. Kohno, and X. Hu, Phys. Rev. Lett. **94**, 087205 (2005).

<sup>23</sup> J. S. Lee, M. W. Kim and T. W. Noh, New J. Phys. **7**, 147 (2005).